Monthly Notices of the ROYAL ASTRONOMICAL SOCIETY

MNRAS **464,** 3090–3100 (2017) doi:10.1093/mnras/stw2573
Advance Access publication 2016 October 10

MOCCA-SURVEY Database I: Is NGC 6535 a dark star cluster harbouring an IMBH?

Abbas Askar,[1]★ Paolo Bianchini,[2]★ Ruggero de Vita,[3] Mirek Giersz,[1] Arkadiusz Hypki[4] and Sebastian Kamann[5]

[1]*Nicolaus Copernicus Astronomical Centre, Polish Academy of Sciences, ul. Bartycka 18, PL-00-716 Warsaw, Poland*
[2]*Max-Planck Institute for Astronomy, Koenigstuhl 17, D-69117 Heidelberg, Germany*
[3]*School of Physics, University of Melbourne, VIC 3010, Australia*
[4]*Leiden Observatory, Leiden University, PO Box 9513, NL-2300 RA Leiden, the Netherlands*
[5]*Institut für Astrophysik, Georg-August-Universität Göttingen, Friedrich-Hund-Platz 1, D-37077 Göttingen, Germany*

Accepted 2016 October 5. Received 2016 October 3; in original form 2016 July 27; Editorial Decision 2016 October 3

ABSTRACT

We describe the dynamical evolution of a unique type of dark star cluster model in which the majority of the cluster mass at Hubble time is dominated by an intermediate-mass black hole (IMBH). We analysed results from about 2000 star cluster models (Survey Database I) simulated using the Monte Carlo code MOnte Carlo Cluster simulAtor and identified these dark star cluster models. Taking one of these models, we apply the method of simulating realistic 'mock observations' by utilizing the Cluster simulatiOn Comparison with ObservAtions (COCOA) and Simulating Stellar Cluster Observation (SISCO) codes to obtain the photometric and kinematic observational properties of the dark star cluster model at 12 Gyr. We find that the perplexing Galactic globular cluster NGC 6535 closely matches the observational photometric and kinematic properties of the dark star cluster model presented in this paper. Based on our analysis and currently observed properties of NGC 6535, we suggest that this globular cluster could potentially harbour an IMBH. If it exists, the presence of this IMBH can be detected robustly with proposed kinematic observations of NGC 6535.

Key words: methods: numerical – stars: black holes – stars: kinematics and dynamics – globular clusters: general – globular clusters: individual: NGC 6535.

1 INTRODUCTION

Observational evidence has proven the existence of both stellar mass black holes (BHs) and supermassive BHs. However, no conclusive evidence has been found for the presence of BHs that have masses in the range of 10^2–$10^5 M_\odot$. This elusive mass range for BHs classifies intermediate-mass black holes (IMBHs). There are few plausible formation scenarios for IMBHs. They could be remnants of hypothesized metal-free Population III stars that formed in the early Universe (Madau & Rees 2001) or they may form via dynamical processes in star clusters (e.g. Miller & Hamilton 2002; Gürkan, Freitag & Rasio 2004; Portegies Zwart et al. 2004; Giersz et al. 2015). Therefore, the presence of IMBH in globular clusters (GCs) has been the subject of considerable debate (Sun et al. 2013; Lützgendorf et al. 2016, and reference therein).

Along with dynamical formation scenarios for IMBH in dense stellar environments, the extrapolation of correlations between supermassive BHs and the masses of their host galaxies to lower mass systems like GCs suggests that IMBHs could be present in massive clusters (Magorrian et al. 1998; Ferrarese & Merritt 2000; Graham & Scott 2015).

The prevalent methods for detecting IMBH in GCs involve kinematic observations of stars near the cluster centre or searching for electromagnetic radiation from matter accretion on to an IMBH (Strader et al. 2012, and references therein). The presence of an IMBH should have a distinct signature in the line-of-sight velocity dispersion profile from stars close to the IMBH (Gebhardt et al. 2000; Gerssen et al. 2002, 2003; Noyola, Gebhardt & Bergmann 2008; Lützgendorf et al. 2011), namely a rise in the central velocity dispersion (Bahcall & Wolf 1976). This method for detecting IMBH is particularly challenging as observing central regions of extremely dense stellar environments like GCs requires instruments with high spatial resolution and accurate velocity measurements (Bianchini et al. 2016; de Vita et al. 2016). Due to the difficulties and uncertainties in measuring the central velocity dispersions of GCs, there have been contradictory results regarding whether or not certain Galactic GCs harbour an IMBH. Certain kinematic

★ E-mail: askar@camk.edu.pl (AA); bianchini@mpia-hd.mpg.de (PB)

observational techniques like integrated light spectroscopy show rising central velocity dispersions for GCs, while resolved stellar kinematics do not confirm this signature associated with the presence of an IMBH (for the specific case of the GC NGC 6388, see Lützgendorf et al. 2011, 2015 and Lanzoni et al. 2013; for ω Cen, see Anderson & van der Marel 2010 and Noyola et al. 2010). Due to these contradictory results, the detection of IMBH in GCs remains controversial.

In this paper, we discuss the dynamical evolution of a unique type of star cluster model that emerged from around 2000 models simulated using the MOnte Carlo Cluster simulAtor (MOCCA) code as part of the Survey Database I project (Askar et al. 2017). Very early in their dynamical evolution, these clusters form an IMBH via the formation scenario proposed by Giersz et al. (2015). The IMBH mass continues to grow during the cluster evolution and within a Hubble time, the IMBH becomes the dominant mass in the system making up for at least 50 per cent of the total cluster mass. Banerjee & Kroupa (2011) introduced the term 'dark star clusters' (DSCs) in their work describing the evolution of cluster models with low Galactocentric radius values. In the clusters described by Banerjee & Kroupa (2011), the stars in the outer part would rapidly escape due to tidal stripping leaving a compact cluster held together by a BH subsystem. In the DSC model discussed in this paper, the majority of the mass of the DSC is in the IMBH and is not attributed to the presence of a BH subsystem or a large population of other dark remnants. Recent kinematic observations by Taylor et al. (2015) of more than a hundred GCs in the giant elliptical galaxy NGC 5128 have revealed high mass-to-light (M/L) ratio values for several of these extragalactic GCs. These observational results point towards the presence of a significant dark mass component in these clusters that could potentially be explained by the presence of an IMBH or a subsystem of compact remnants.

In this paper, we provide a detailed and comprehensive description of the observable photometric and kinematic properties of our DSC model, using the strategy of simulating mock observations. This enables us to put forward a direct comparison between models and real data. We find that the observable properties of the DSC model at Hubble time are particularly close to the peculiar Galactic GC NGC 6535 (Halford & Zaritsky 2015). We investigate the possibility that NGC 6535 followed an evolution similar to the DSC model described in this paper and we suggest that it could be a potential candidate for harbouring an IMBH. The kinematic signature of an IMBH in this relatively small cluster would be easier to detect compared to larger and more massive Galactic GCs and suggested kinematic observations of NGC 6535 may provide clear-cut evidence for the presence of an IMBH in certain GCs. We would like to explicitly state that the DSC model presented in this paper was not specifically tailored to reproduce NGC 6535; however, at 12 Gyr, it has observational properties remarkably similar to NGC 6535.

In Section 2, we briefly describe the MOCCA code for star cluster simulations, the Cluster simulatiOn Comparison with ObservAtions (COCOA) and Simulating Stellar Cluster Observation (SISCO) codes used to simulate observational data for our simulated cluster model. We provide the details of the evolution of the DSC model that we simulated with MOCCA and use mock observations to compare the properties of this model with the Galactic GC NGC 6535 in Section 3. Sections 4 and 5 show the results of the simulated observations of our cluster model from COCOA and SISCO and we further discuss the possibility of observing an IMBH in NGC 6535 in Section 5. In Section 6, we present the main conclusions and discussion of our results.

2 METHOD

2.1 MOCCA

The MOCCA code is a numerical simulation code for long-term evolution of spherically symmetric star clusters. MOCCA is based on Hénon's Monte Carlo method (Hénon 1971) that was subsequently improved by Stodółkiewicz in the early 1980s (Stodółkiewicz 1986) and later by Giersz and his collaborators (see Giersz et al. 2013, and references therein for a description of MOCCA and the Monte Carlo Method). The Monte Carlo method can be regarded as a statistical way of solving the Fokker–Planck equation in which the cluster is represented as a set of particles. The basic underlying assumptions for the Monte Carlo method are that the cluster needs to be spherically symmetric and that its evolution is driven by two-body relaxation. These assumptions allow the Monte Carlo method to compute the cluster evolution much faster than *N*-body codes and the implementation of this method allows inclusion of additional physical effects. In addition to relaxation, which drives the dynamical evolution of the system, MOCCA includes prescriptions for synthetic stellar evolution of all single and binary stars in the system provided by Hurley, Pols & Tout (2000) and Hurley, Tout & Pols (2002) (BSE code). MOCCA also uses direct integration procedures for small *N* sub-systems using the FEWBODY code (Fregeau et al. 2004). This allows it to accurately model interactions and encounters between different objects. A realistic treatment of escape processes in tidally limited clusters based on Fukushige & Heggie (2000) has been implemented in the code.

MOCCA has been extensively tested against the results of *N*-body simulations of star clusters comprising of thousands up to a million stars (Giersz et al. 2013; Heggie 2014; Giersz et al. 2015; Mapelli 2016; Wang et al. 2016, and references therein). The agreement between the results from these two different types of simulations is excellent. This includes the global cluster evolution, mass segregation time-scales, treatment of primordial binaries (energy, mass and spatial distributions) and the number of retained neutron stars, BHs and other exotic objects. The output from MOCCA code is as detailed as direct *N*-body codes, but MOCCA is significantly faster than *N*-body codes and can simulate a realistic GC within a day.

The speed of MOCCA makes it ideal for simulating a large number of models with different initial conditions. The DSC model presented in this paper was among 1948 models that were simulated as part of the MOCCA Survey I project (Askar et al. 2017; Belloni et al. 2016). These models cover a wide range of the initial parameter space with different star numbers, metallcities, binary fractions, central densities etc. The details of the initial parameters for the models simulated in MOCCA Survey I data base can be found in table 1 of Askar et al. (2017). The initial conditions for these models were selected arbitrarily to cover a wide range of parameter space and were not selected to reproduce particular cluster models. However, observational properties of the cluster models at Hubble time can reproduce observed properties of most Galactic GCs. A description of the models simulated in the Survey I project can be found in Askar et al. (2017).

2.2 COCOA

To simulate photometric optical observations of our DSC model, we utilize the COCOA code (Askar et al. 2016). The COCOA code is being developed to extend numerical simulations of star clusters for direct comparisons with observations. As an input, it uses the snapshots produced by Monte Carlo or *N*-body simulations. The

Table 1. Initial parameters of the simulated dark star cluster model.

N	Mass ($M_\odot$)	Binary fraction	Z	IMF	Central density ($M_\odot$ pc^{-3})	r_h (pc)	r_t (pc)	R_{GC} (kpc)	Fallback
400 000	2.42×10^5	10 per cent[a]	0.001	2[b]	3.85×10^6	1.20	30.0	1.94	On[c]

Notes. [a]The semimajor axis distribution for primordial binaries is uniform in Log(a) with maximum semimajor axis value being 100 au. Mass ratio (q) distribution was uniform for primordial binaries and the eccentricity distribution was thermal.
[b]2 indicates that the cluster had a two segment initial mass function as given by Kroupa (2001). The initial masses of the stars were distributed between 0.08 and 100$M_\odot$. r_h and r_t give the initial intrinsic half-mass radius and tidal radius, respectively. R_{GC} is the Galactocentric radius of the dark star cluster model.
[c]BH kicks are treated with the mass fallback prescription given by Belczynski, Kalogera & Bulik (2002).

snapshots from MOCCA code contain information about the positions, velocities, stellar parameters and magnitudes of all objects in the star cluster at a specific time during the cluster evolution. Using the simulation snapshot, COCOA projects numerical data on to the plane of the sky and can create observational data in the form of FITS files. The distance to the cluster, exposure time, resolution and other instrumental specifications for the simulated observational data obtained from COCOA can be adjusted by the user to recreate observations from virtually any telescope (Askar et al., in preparation).

2.3 SISCO

To produce a mock kinematic observation of our DSC, we apply the software SISCO described in Bianchini et al. (2015). The software simulates Integral Field Unit (IFU) observations of stellar systems starting from a dynamical simulation of star clusters and it is optimized to read as an input the projected cluster snapshot derived from the COCOA software. It assigns to every star a stellar spectrum, based on the stellar parameters, in the waveband of the Ca triplet (8400–8800 Å) with a resolving power $R \approx 20\,000$ (properties similar to typical IFU instruments like FLAMES@VLT in ARGUS mode). Then, the instrumental setup is customized, including the size of the field of view (FOV), the spaxel scale, point spread function (PSF) shape, seeing conditions, signal to noise. The output of the code is a three-dimensional data cube in which each spatial pixel has an assigned spectrum and luminosity information.

3 THE SIMULATION MODEL: DSC

From the MOCCA Survey I simulation models, there were 344 models out of 1948 that formed an IMBH (with mass greater than 150 $M_\odot$) within 12 Gyr of cluster evolution. From these 344 models, we found 42 models in which the IMBH mass makes up for at least 50 per cent of the total cluster mass after 12 Gyr of evolution. We categorize these models as DSCs harbouring an IMBH. The 42 DSC models emerge from models with diverse initial conditions for parameters such as number of objects ($N = 4 \times 10^4$, 1×10^5, 4×10^5, 7×10^5, 1.2×10^6), metallicity ($Z = 0.0002$, 0.001, 0.005, 0.006, 0.02), binary fraction (0.05, 0.1, 0.3, 0.95) and initial concentration (initial King concentration parameter $W_0 = 3$, 6, 9). 74 per cent of the DSC models had high initial concentrations (with $W_0 = 9$) and initial half-mass radius less than 1.5 pc. All 42 DSC models from the survey data base have small Galactocentric distance values ranging from 1.1 up to 5 kpc. Most of these DSCs models are also characterized by sufficiently small half-mass relaxation times with about 80 per cent of the cluster models having initial half-mass relaxation times less than 400 Myr. Furthermore, in more than 80 per cent DSC models, an IMBH of 150 $M_\odot$ forms within 100 Myr of cluster evolution through the fast scenario described in Giersz et al. (2015). These general trends in the initial properties of the DSC model are easy to understand. First, an IMBH needs to form early enough in the cluster evolution so that its mass can grow significantly; for these low half-mass relaxation times, high central density and concentration are needed. Secondly, a large number of stars need to escape the cluster due to tidal stripping; for this reason, the cluster needs to have a small Galactocentric distance value. Only in 2 DSC models did the IMBH form after 400 Myr of evolution; in one model, the IMBH formed close to 800 Myr, while in the other one, the IMBH formed after about 5.8 Gyr of cluster evolution via the slow scenario explained in Giersz et al. (2015).

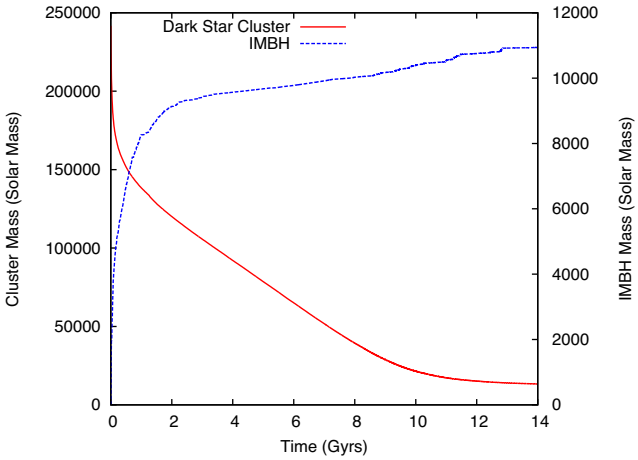

Figure 1. The solid line shows the evolution of the total mass of the cluster with time. The mass of the cluster decreases almost constantly between 2 and 10 Gyr of cluster evolution. The dashed line shows the build-up of the IMBH mass with time (please refer to the second y-axis for the label for this line). It can be seen that the IMBH mass rapidly increases during the first 2 Gyr of cluster evolution.

To carry out a more detailed investigation of the evolution of a DSC model and the influence of an IMBH on the observable properties of such clusters at 12 Gyr, we selected a model that had initial conditions representative of most DSC models that emerged in the survey data base. The selected model was the most massive model at 12 Gyr in which the mass of the IMBH at 12 Gyr made up for at least 70 per cent of the cluster mass. This particular DSC has initially $N = 400\,000$ objects with 10 per cent primordial binary fraction. The initial mass of the cluster model is 2.4×10^5 $M_\odot$, with a very high central density of 3.85×10^6 $M_\odot pc^{-3}$ and a King concentration parameter value of $W_0 = 9$. The cluster is initially underfilling at a Galactocentric radius of 1.94 kpc. At 12 Gyr, the mass of the cluster is reduced to 1.5×10^4 $M_\odot$. The evolution of the cluster mass with time up to 14 Gyr is shown in Fig. 1. Important initial parameters of the cluster model are given in Table 1.

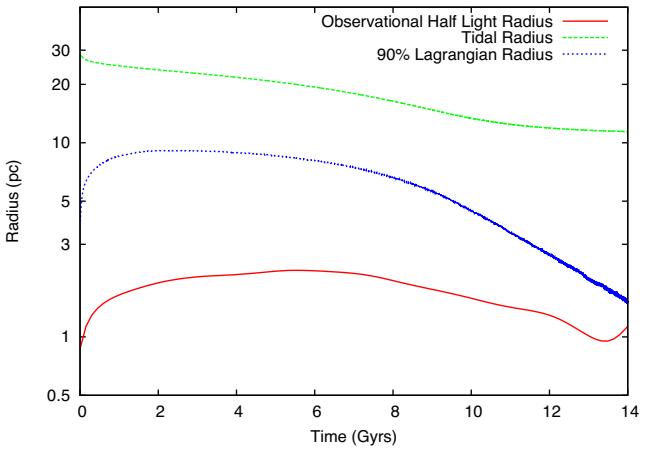

Figure 2. The figure shows the evolution of the 3D tidal radius, observational 2D half-light radius and the 3D 90 per cent Lagrangian radius of the dark star cluster model with time.

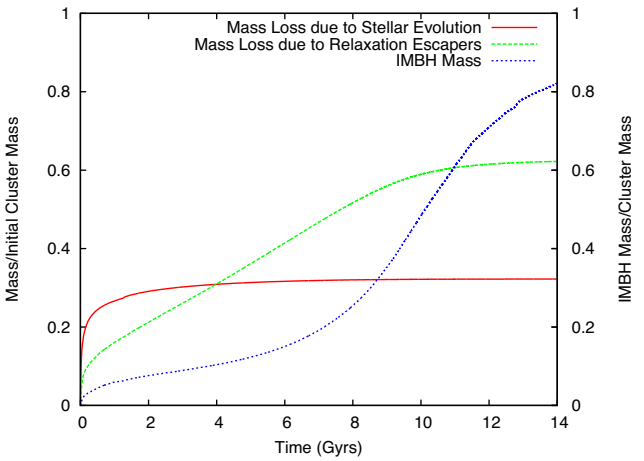

Figure 3. The solid and dashed lines in the figure show the ratio between mass-loss due to different processes (escapers and stellar evolution) and initial cluster mass. The primary mechanism for mass-loss in the dark star cluster model is due to stars escaping because of relaxation after 4 Gyr of clusters evolution. The dotted line shows the ratio between IMBH and cluster mass at that time (please refer to the second *y*-axis).

The minimum and maximum initial stellar masses in the simulated model were 0.08 and 100 $M_\odot$.

The formation of the IMBH in this model is connected with the fast scenario that is explained in Giersz et al. (2015). Here we describe the process of the formation of the IMBH during the early evolution of this particular DSC model. The very dense initial model results in multiple collisions between main sequence (MS) stars (Portegies Zwart et al. 2004; Mapelli 2016) that eventually result in the formation of a massive MS star of 377 $M_\odot$. This massive MS star undergoes a direct collision with a BH of 195 $M_\odot$ that formed from the evolution of another massive MS star that also underwent mass buildup due to collisions with other stars and mergers in binary interactions. This direct collision between the 377 $M_\odot$ MS star and the 195 $M_\odot$ BH resulted in the formation of a very massive seed BH in the cluster of 572 $M_\odot$ within 9 Myr of cluster evolution. It is assumed that 100 per cent of the MS star is accreted on to the BH following a direct collision. This is a rather unrealistic assumption; however, even with less than 50 per cent of the MS mass being accreted on to a BH, a massive IMBH seed will still be formed (Giersz et al. 2015). The mass of the IMBH grows to 1.08×10^4 $M_\odot$ at 12 Gyr, making up for more than 70 per cent of the cluster mass at this time.

The IMBH continues to gain mass during the evolution of the system, as shown in Fig. 1. The IMBH rapidly gains mass during the first 2 Gyr of cluster evolution mainly via collisions with other stars and compact objects and mergers after binary-single and binary–binary interactions. Due to the high initial density, numerous interactions between the stars in the cluster takes place during the first 100 Myr of cluster evolution that contributes to the very high rate of IMBH mass build-up.

Mass -loss due to stellar evolution of massive stars and the formation of an IMBH in this dense system results in the expansion of the half-light radius (Fig. 2) during the first 5 Gyr of cluster evolution (the radius increases from 1.2 to 3.65 pc). Due to the small tidal radius of the cluster, a lot of stars escape the cluster due to tidal stripping and relaxation. After 5 Gyr of evolution, the half-light radius starts to decrease as tidal stripping takes over the expansion connected to energy generated in the cluster core and the size of the cluster decreases. Escaping stars become the dominant mass-loss mechanism for the cluster as the tidal radius of the cluster further decreases. Tidal stripping results in the escape of a large number of objects from the system, with a nearly constant rate until 10 Gyr. At this time, the IMBH mass is about 50 per cent of the current cluster mass and there are not many stars left in the outer parts of the cluster that would escape easily (see evolution of the 90 per cent Lagrangian radius in Fig. 3). The cluster becomes tidally underfilling again and the rate at which stars are escaping decreases significantly (Fig. 3). Table 2 reports the relevant properties of the DSC at 12 Gyr.

3.1 Closest target: NGC 6535

We compared various properties of our simulated DSC model with the properties of Galactic GCs in the Harris catalogue (Harris 1996, updated 2010). Starting from the comparison of the cluster mass and half-light radius, we found that the DSC model simulated with MOCCA has observational properties at 12 Gyr that are similar to the Galactic GC NGC 6535. This is a particularly interesting GC. Halford & Zaritsky (2015) have described NGC 6535 to be 'sufficiently perplexing', because of its high dynamical M/L ratio (Zaritsky et al. 2014) and its present-day mass function that is 'unusually bottom-light' (Halford & Zaritsky 2015). We would like to stress that the simulated DSC model was not meant to replicate or directly model NGC 6535, but it displays remarkable similarity with the observational properties of this Galactic GC. The comparison between the DSC model and NGC 6535 is summarized below.

(i) The estimated half-light radius for NGC 6535 is 1.68 pc (Watkins et al. 2015). The observed half-light radius of our DSC model at 12 Gyr is 1.5 pc.

(ii) The core radius of NGC 6535 is 0.71 pc and the concentration parameter c is 1.33, giving a tidal radius of 15.3 pc. The tidal radius for the DSC model at 12 Gyr is 11.9 pc.

(iii) The position of the selected DSC model is in close proximity to NGC 6535 when plotted on a cluster mass versus half-light radius plot of all Galactic GCs. This can be seen in Fig. 4. For all DSC models in which the IMBH makes up a significant fraction (more than 70 per cent) of cluster mass at 12 Gyr, the model presented in this paper has mass and half-mass radii that is closest to NGC 6535. The cluster mass for Galactic GCs was calculated using the absolute

Table 2. Parameters of the simulated dark star cluster model at 12 Gyr taken directly from the MOCCA simulation. Values of significant scale radii are also provided in units of arcseconds assuming that the dark star cluster is at a distance of 6800 pc from the Sun.

N	Mass ($M_\odot$)	Binary fraction	Central density ($M_\odot pc^{-3}$)	r_c pc (arcsec)	r_{hl} pc (arcsec)	r_t pc (arsec)	IMBH mass ($M_\odot$)
8294	1.51×10^4	5.8 per cent	1.30×10^7	0.17 (5.16 arcsec)	1.5 (45.5 arcsec)	11.92 (361.6 arcsec)	1.08×10^4

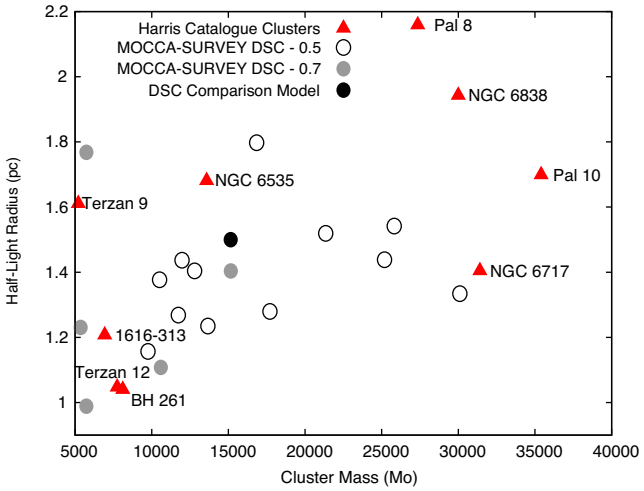

Figure 4. Mass versus half-light radius plot for Galactic GCs (red triangles) taken from the Harris (1996, updated 2010) catalogue and dark star cluster models in the MOCCA-Survey data base. Open circles show dark star cluster models in which the IMBH mass is larger than 50 per cent but less than 70 per cent of the total cluster mass at 12 Gyr. The grey circles show dark star cluster models in which the IMBH makes up for more than 70 per cent of the cluster mass at 12 Gyr. The filled black circle represents the dark star cluster model presented in this paper. This model has the closest proximity to NGC 6535 for the models in which the IMBH mass is more than 70 per cent of the total cluster mass.

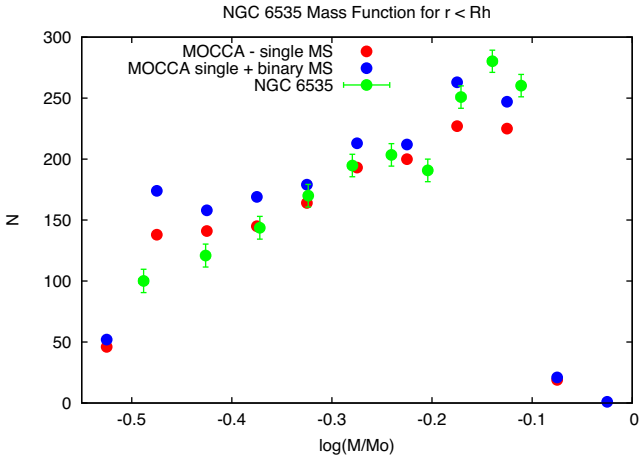

Figure 5. The figure above shows the mass function for NGC 6535 obtained by Halford & Zaritsky (2015) with solid black circles points. The mass function obtained from the dark star cluster model of MOCCA is shown by unfilled circles (single stars only) and grey (including binaries) points. The numbers of stars have been scaled to see the similarity in the shape of the mass function.

visual magnitude (M_V) and assuming that the M/L is 2 (this is a conservative assumption for NGC 6535).

(iv) NGC 6535 has a particularly high M/L ratio value of about 11 (Zaritsky et al. 2014). To check whether NGC 6535 may have had a bottom-heavy initial mass function (IMF), Halford & Zaritsky (2015) used *Hubble Space Telescope* (*HST*) data to measure the present-day stellar mass function of NGC 6535 and found a dearth of low-mass stars in the cluster. We were able to obtain the mass function of our DSC model using the simulation snapshot at 12 Gyr. The shape of the mass function from the DSC model is comparable to the mass function obtained by Halford & Zaritsky (2015), as presented in Fig. 5. To compare the mass function from the simulation data with the observed mass function and to mimic the observational biases, we took data for single MS stars (plotted in red in Fig. 5) and we also computed the mass function by including binaries with MS stars and compact object companions and MS–MS binaries that have mass ratio (q) less than 0.5 (shown by blue points in Fig. 5). The high M/L ratio of NGC 6535 and a bottom-light mass function suggest the presence of a significant dark component in this cluster. This dark component could comprise of a large number of compact objects (Banerjee & Kroupa 2011) like a BH subsystem (Wang et al. 2016) or it could be an IMBH. Moreover, it has been suggested by Hurley (2007) that if the ratio between the core and the half-mass radius of a star cluster is larger than 0.5, then 'something out of the ordinary' may be needed to explain the inner structure of such a star cluster model. NGC 6535 is one of the six GCs in our Galaxy in which this ratio is larger than 0.5.

The Galactocentric radius of NGC 6535 is 3.9 kpc and it is in close proximity to the Galactic bulge. NGC 6535 has a larger Galacotcentric radius (3.9 kpc) compared to the DSC model (1.94 kpc). However, it is possible that NGC 6535 may have followed a similar evolution to the DSC model despite having a higher Galactocentric radius. This is because the actual Galactic potential is more complicated than the point mass approximation used in MOCCA. Thus, the actual Galactic potential may have a stronger influence on the dynamical evolution of NGC 6535, comparable to the influence that a point mass Galactic potential would have on a cluster with lower Galactocentric radius and a circular orbit (Madrid et al. 2016). Moreover, if NGC 6535 has an elliptical orbit, then the strong influence of the Galactic potential during pericentre passages may also make the evolution of NGC 6535 similar to the DSC model. Halford & Zaritsky (2015) remark that it has been suggested by Paust et al. (2009) that some clusters with close proximity to the Galactic bulge (like NGC 6535) may undergo tidal stripping of low-mass stars that could explain the present-day mass function of NGC 6535.

The absolute visual magnitude of the DSC model at 12 Gyr is −4.162 and the observed magnitude of the NGC 6535 is −4.75. The binary fraction for NGC 6535 derived by Milone et al. (2012) is 0.066 ± 0.018 and the binary fraction for the DSC model is 0.058. The observational parameters of NGC 6535 match reasonably well with the parameters derived from the synthetic observations of the DSC model. This suggests that NGC 6535 could be a reasonably good candidate for harbouring an IMBH. Other detailed structural and kinematic similarities between the simulated DSC model and NGC 6535 are further discussed in the subsequent sections.

4 MOCK PHOTOMETRY WITH COCOA

We used the COCOA code in order to simulate idealized synthetic observations of the DSC model and carry out PSF photometry on

Figure 6. Left-hand panel: mock observation of the dark star cluster model with an 8-m class telescope (FOV: 2.73 × 2.73 arcmins). The image was created using COCOA and the 12 Gyr MOCCA snapshot for the cluster model. The RGB image was obtained by combining synthetic observations in the *I*, *V* and *B* filters. The model was projected at a distance of 6.8 kpc in order to compare it with NGC 6535. Right-hand panel: Hubble Image of NGC 6535 from four different filters (FOV: 3.31 × 3.28 arcmins).[1]

Table 3. Parameters of the instrument for simulated COCOA images. The *V*-band exposure was 100 times the fraction of direct counts.

Image size	2048 × 2048 pix
Distance	6.8 kpc
Pixel scale	0.08 arcsec pix^{-1}
Seeing	0.3 arcsec
PSF	Moffat
GAIN	1.2
Noise	On

the simulated images. To compare our DSC model with NGC 6535, we took the simulation snapshot at 12 Gyr and projected it at a distance of 6.8 kpc. To carry out mock photometry of the simulated model, observations of the cluster were simulated with a high spatial resolution optical telescope (8 m-class) that had a pixel scale of 0.08 arcsec pixel^{-1}. The projected snapshot contained magnitudes for all stars in *B*, *V* and *I* filters; each of these filters was used to simulate separate observations of the DSC model. The left-hand panel in Fig. 6 shows the composite red giant branch (RGB) image of the DSC model that was produced with COCOAusing three separate observations in three different filters. The right-hand panel of Fig. 6 shows an *HST* image of NGC 6535. It can be seen from the figure that the spatial structure of the DSC model at 12 Gyr is similar to the *HST* image of NGC 6535. The parameters of the instrument with which the observations are simulated with COCOA are given in Table 3.

4.1 CMD for the cluster model at 12 Gyr

We carried out PSF photometry on the simulated *B*-, *V*- and *I*-band images to create a catalogue of all stars that could be observed in the cluster model. This was done by employing the automated photometry pipeline in COCOA that utilizes DAOPHOT/ALLSTAR (Stetson 1987, 1994) to do PSF photometry. By making use of the photometric catalogues from the simulated observation, we were able to obtain the observed colour–magnitude diagrams (CMDs) for our DSC model. We created $B-V$ versus V and $V-I$ versus V CMDs. Fig. 7 shows $V-I$ versus V CMD obtained for the DSC model with red points. The instrumental magnitudes obtained from COCOA have been converted to absolute magnitudes. The CMDs show a lack of horizontal branch stars. There are also very few evolved giant stars left in the cluster.

The CMD results for the DSC model is compared with observational CMD of NGC 6535 for which the data were obtained through the Rosenberg early ground-based survey (Rosenberg et al. 2000a,b; Piotto et al. 2002). Photometric data for NGC 6535 were available in *V* and *I* filters. The CMD with colour $V-I$ versus V is plotted from ground-based observations of NGC 6535 with green points along with the data from the mock photometry done with COCOA in Fig. 7. The photometric data for NGC 6535 were restricted to stars for which the magnitude error was less than 0.3 and the apparent magnitudes were converted to absolute magnitudes and corrected for reddening. The CMD for NGC 6535 and the DSC model match very well and show how closely the DSC model at 12 Gyr resembles NGC 6535. The $V-I$ colours for NGC 6535 are bluer than the one for the DSC model. The derived metallicity for NGC 6535 is an order of magnitude lower than the metallicity for the simulated DSC model. The CMD obtained from the photometry of the DSC model also closely matches with the CMD from Hubble for NGC 6535 provided in fig. 1 of Halford & Zaritsky (2015). The difference in metallicity and age of NGC 6535 compared to the 12 Gyr snapshot for the DSC model accounts for the small differences between the two CMDs. In order to check whether decreasing the metallicity would significantly influence the evolution of the DSC model, we simulated the same initial model with a metallicity of $Z = 3.24 \times 10^{-4}$ and found that the cluster follows a very similar evolution to the higher metallicity model. The lower metallicity cluster also goes on to form an IMBH that dominates the cluster mass. The half-light radius and mass function of the lower metallicity cluster model at 10.5 Gyr (estimated age of NGC 6535 taken from Marín-Franch et al. 2009) is comparable to properties of the $Z = 0.001$ DSC model at 12 Gyr.

[1] Link: http://www.spacetelescope.org/images/potw1452a/Credit: ESA/Hubble and NASA, Acknowledgment: Gilles Chapdelaine.

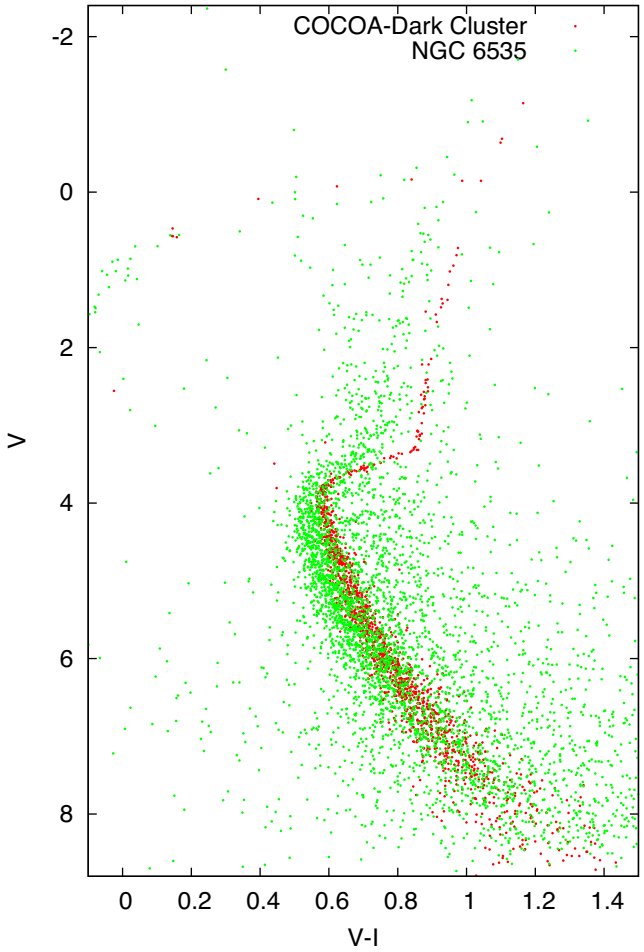

Figure 7. $V-I$ versus V colour–magnitude diagram for the dark star cluster model (grey points, obtained after simulating observations with COCOA) and NGC 6535 (black points taken from ground-based observations (Piotto et al. 2002)[2]. The magnitudes are absolute and the observational data have been corrected for extinction. The CMD from NGC 6535 shows that stars are bluer. This can be attributed to the lower metallicity and relatively younger age of NGC 6535.

4.2 Surface brightness profile

The surface brightness profile for the DSC model at 12 Gyr is shown in Fig. 8. To compare with NGC 6535, the cluster was projected at a distance of 6.8 kpc. The surface brightness profile for our DSC model declines steeply after the radius of 30 arcsec. The surface brightness profile was fit to the single mass King model to obtain cluster parameters from the projected snapshot. The core radius (r_c) obtained from the King fitting is 0.53 pc (16 arcsec). The half-light radius is 1.24 pc (37.8 arcsec). Please see Table 4 for the derived observational parameters for the DSC model and NGC 6535. For comparison, we took the surface brightness profile for NGC 6535 obtained by Noyola & Gebhardt (2006) using *HST* observations. Noyola & Gebhardt (2006) remark that their observations of NGC 6535 contained very few stars and the measured profile was very noisy. The steepness in the observed surface brightness profile of NGC 6535 is similar to the steepness and shape of the profile of the DSC model with a shift of about 1 mag arcsec^2

[2] Link: http://groups.dfa.unipd.it/ESPG/NGC6535.html University of Padova, Stellar Populations Database

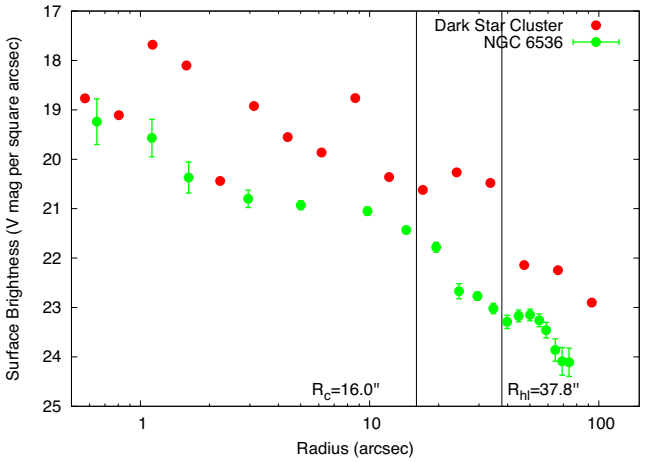

Figure 8. The dark grey points show the surface brightness profile for the dark star cluster model at 12 Gyr. The *y*-axis shows the absolute *V*-band magnitude per square arcseconds (for the cluster projected at 6.8 kpc) and the *x*-axis shows the distance from the centre in arcseconds. The vertical lines in the graph indicate the observed positions of the core and half-light radii. The light grey points show the surface brightness profile for NGC 6535 obtained by Noyola & Gebhardt (2006).

for points beyond 1 arcsec. The core radius and the break radius obtained by Noyola & Gebhardt (2006) from the surface brightness profile gives values of 1.7 arcsec (0.06 pc) and 21.2 arcsec (0.70 pc) that are significantly smaller than more recently observed core and half-light radii for NGC 6535 (Harris 1996, updated 2010).

We attempted to fit the surface brightness and velocity dispersion profile of the DSC model at 12 Gyr to the single-mass King model (King 1966) to obtain cluster parameters. Fitting single-mass models has been one of the standard procedures used by observers to obtain cluster parameters. However, due to the presence of an IMBH, fitting both the profiles together was difficult and a reasonable goodness of fit value was not achieved. The presence of a massive compact object or a compact object subsystem in the cluster can result in this difficulty in fitting the King (1966) model to the profiles. This problem was also reported and explained by Wang et al. (2016) for their clusters that had a presence of a large BH subsystem. In the next section, we will describe how the presence of the IMBH in our DSC model significantly influences the kinematic structure, in particular, the velocity dispersion profile.

5 MOCK KINEMATICS WITH SISCO

Before we explore the details of the kinematics of our simulated cluster, we compare the velocity dispersion profiles (VDP) available in the literature for NGC 6535 with the one obtained from our simulation. The most recent and complete kinematic data of NGC 6535 are the *HST* proper motions presented in Watkins et al. (2015) (see also Bellini et al. 2014). We construct the dispersion profiles (both for the line of sight and proper motions) from our simulation considering all the stars brighter than 20.1 mag in the *HST F606W* filter, in agreement with the procedure followed by Watkins et al. (2015). Fig. 9 shows the observed dispersion profile and the profile from our simulation. While observational data are missing for the inner 10 arcsec on the cluster, a good agreement is observed at larger radii. Other spectroscopic studies report values of integrated-light velocity dispersion within the half-light radius of $3.27^{+0.67}_{-0.53}$ km s^{-1} (Zaritsky et al. 2014) consistent with the outer values of our profiles and the profile measured by Watkins et al. (2015). Moreover, Watkins et al. (2015) find significant radial

Table 4. Current observational parameters for the NGC 6535 model and parameters for the dark star cluster (DSC) model at 12 Gyr from MOCCA and COCOA.

	σ_0 (km s^{-1}) [a]	c [b]	Core radius (pc)	Half-light radius (pc)	M/L ratio
NGC 6535	2.40 ± 0.5 [c]	1.33 ± 0.16	0.71 (21.6 arcsec)	1.68 (51.0 arcsec)	$11.06^{+2.68}_{-2.12}$ [d]
DSC model (MOCCA)	37.3	1.85	0.17 (5.16 arcsec)	1.5 (45.5 arcsec)	3.83
DSC model-COCOA King Fit-SBP [e]	x	1.25	0.52 (16.0 arcsec)	1.24 (37.8 arcsec)	x
DSC model-SISCO	15–25 km s^{-1}	x	x	x	17

Notes. [a]σ_0 is the central velocity dispersion in units of km s^{-1}.
[b]c defines the concentration parameter given by $\log_{10} \frac{r_t}{r_c}$, where r_t is tidal radius and r_c is the core radius.
[c]Observed value of the central velocity dispersion taken from the Harris catalogue (Harris 1996, updated 2010). The observed values for central velocity dispersion are derived from observations of stars further out from the centre of the cluster.
[d]The observed mass-to-light ratio for NGC 6535 is taken from Zaritsky et al. (2014).
[e]Parameters obtained from King model fitting of the surface brightness profile only.

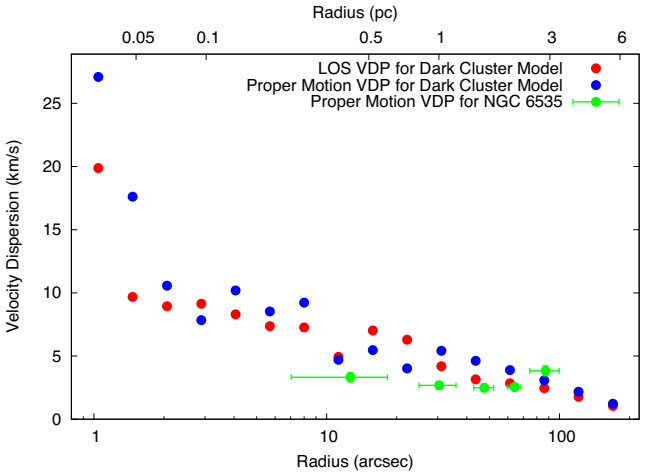

Figure 9. The figure shows the comparison between the dispersion profiles for the dark star cluster model at 12 Gyr and available observable dispersion profile for NGC 6535. The grey and unfilled circles show the line-of-sight velocity dispersion and proper motion dispersion for the dark star cluster model, black points represent the proper motion dispersion data for NGC 6535 obtained from Watkins et al. (2015). The dark star cluster model data were restricted to the same limiting magnitude used by Watkins et al. (2015). Proper motion dispersion values between 30 and 70 arcsec are comparable for NGC 6535 and the dark star cluster model.

anisotropy for NGC 6535, $\sigma_t/\sigma_r \approx 0.79$; this is the ratio of the tangential dispersion and radial dispersion on the plane of the sky. Our DSC model is also characterized by a mild radial anisotropy ($\sigma_t/\sigma_r \approx 0.97$) when the kinematics is also restricted to the same radial extent and limiting magnitude. However, there is a strong tangential anisotropy in the inner part of the cluster as the average $\sigma_t/\sigma_r \approx 1.40$ within about 1.5 arcsec radius from the cluster centre. This tangential anisotropy close to the IMBH can be seen in the higher position of the proper motion dispersion (blue points) compared to the line-of-sight velocity dispersion (red points) for the three innermost radii in Fig. 9. This strong tangential anisotropy close to the IMBH is in agreement with theoretical studies on the influence of a central BH in star clusters and galaxies (Young 1980; Sigurdsson, Hernquist & Quinlan 1995; Holley-Bockelmann et al. 2002; Hong & Lee 2015).

Given the missing observational information on the kinematics in the central region, we use our software SISCO to simulate integrated-light kinematic measurements. The observational setup used for our mock observation includes a FOV of 20 × 20 arcsec^{-2} (corresponding to ≈0.4 R_h around the centre of the cluster), a spaxel scale of 0.25 arcsec pix^{-1}, a Moffat PSF with seeing of 1 arcsec and a signal-to-noise ratio of 10 for the spectra (see Table 5). Placing the cluster at a distance of 6.8 kpc, a total of 1484 stars fall within the FOV. From the three-dimensional data cube, we extract the velocity dispersion profile, with spatial bins 0.5 arsec wide within the central 2 and 2.0 arcsec wide for the outer parts.[3] For each binned spectra, we extract the velocity dispersion (and associated errors) from line-broadening using the penalized pixel-fitting (PPXF) program of Cappellari & Emsellem (2004). The associated errors and uncertainties for the velocity dispersion measurements are underestimated by the PPXF program. A masking procedure is performed in order to eliminate from the analysis those spaxels that contaminate the kinematics with shot noise (see Bianchini et al. 2015). In particular, we discard from the analysis those spaxels for which one bright star contributes for more than 50 per cent of the total luminosity.

Table 5. Observational setup of the SISCO IFU mock observations.

PSF	Moffat
Seeing	1 arcsec
Spaxel scale	0.25 arcsec pix^{-1}
Field of view	20 × 20 arcsec^{-2}
Signal to noise	10

The centre used for our mock observations with SISCO is the centre of coordinates for an inertial systems that is fixed at the beginning of the MOCCA simulation. There are two important radii connected with the influence of a massive BH in stellar systems, the radius of influence and the wandering radius (Baumgardt, Makino & Ebisuzaki 2004a,b; Amaro-Seoane, Freitag & Spurzem 2004; Stone, Küpper & Ostriker 2016). The radius of influence of the IMBH in the DSC model is about 0.078 pc (2.25 arcsec at an observed distance of 6.8 kpc). The wandering radius that is defined as the offset between the position of the IMBH and the centre of the stellar system for the DSC model is about 0.002 pc or 0.06 arcsec. The definition of the centre represents one of the main observational challenge for a construction of the velocity dispersion profile and it has been shown that it can significantly influence the results (Noyola et al. 2010; van der Marel & Anderson 2010; Bianchini et al. 2015; de Vita et al. 2016). We therefore explore the effect of picking 10 different locations for the centre and construct the corresponding 10 VDP: one for the real

[3] The chosen spatial binning is a trade-off between a high enough spatial resolution of the inner area and high signal to noise.

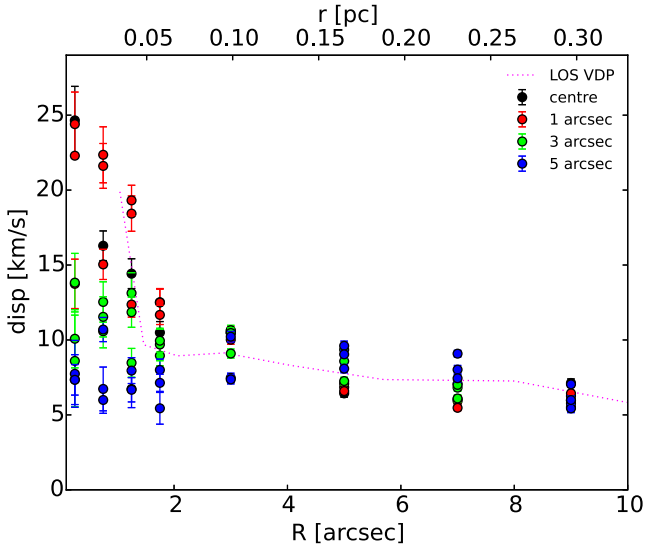

Figure 10. Integrated-light velocity dispersion profiles obtained from our mock observations. 10 velocity dispersion profiles are shown, indicating the 10 different centres used (real centre, three profiles with 1 arcsec offset from the real centre, three profiles with 3 arcsec offsets and three profiles with 5 arcsec offsets). The black points show the velocity dispersion profile when we use the real centre of the cluster. The dotted line indicates the line-of-sight velocity dispersion profile taken directly from the projected simulation snapshot (red points in Fig. 9). Our kinematic mock observations show that the central peak of the velocity dispersion due to the presence of the IMBH is observable.

centre, three at 1 arcsec distance from the real centre, three at 3 arcsec from the real centre and three at 5 arcsec from the real centre. The three different positions of the FOV centre ($(x = 0, y = R)$,$(x = R\sqrt{3/2}, y = -R/2)$ and $(x = -R\sqrt{3/2}, y = -R/2)$) for each radial offset R (1, 3 and 5 arcsec) are separated at a 120° on the circle of radius R. This has been done to have different positions of the centre for each offset in order to avoid any systematic influence that a few bright stars may cause in the velocity dispersion profile calculation.

Fig. 10 shows the dispersion profiles for the different centres, overlapped to the expected profile constructed directly from the simulation. The profiles constructed using the real centre (black points) or a small offset from it (up to 3 arcsec) show a central peak of velocity dispersion, distinctive of the presence of the IMBH, reaching values of 15–25 km s^{-1}. The central rise of the velocity dispersion is erased for a large shift from the real centre (i.e. 5 arcsec), indicating that a careful identification of the centre is needed in order to resolve the central peak. The line-of-sight VDP computed with COCOA from the projected snapshot (Fig. 9) and the SISCO VDP (Fig. 10) are in good agreement. In the next section, we will use the predicted global velocity dispersion in order to calculate the dynamical M/L ratio and we will show how this can be used as an indicator of the presence of the IMBH, independently from the correct identification of the centre.

5.1 Virial estimate of the dynamical M/L

Using the following virial estimate (Wolf et al. 2010)

$$M_{1/2} \simeq 930 \left[\frac{\sigma^2_{\rm los}}{\rm km^2\,s^{-2}}\right]\left[\frac{R_{\rm h}}{\rm pc}\right] {\rm M}_\odot, \quad (1)$$

we can estimate the dynamical mass and dynamical M/L ratio (within the half-light radius) of our simulated cluster based on the kinematic mock observations presented in the previous section. Using a half-light radius of 1.5 pc and an average velocity dispersion of 5 km s^{-1} (lower limit of our mock observations in the central $\approx 0.4R_{\rm h}$ of the cluster[4]), we obtain a mass estimate of $M_{1/2} \simeq 3.5 \times 10^4\,{\rm M}_\odot$. This dynamical mass estimate is consistent within a factor of 2 to the total mass of the 12 Gyr snapshot of our simulation (see Table 2).

Considering a luminosity within the half-light radius of $L_{1/2} = 2000\,{\rm L}_\odot$, we obtain an ${\rm M/L} \simeq 17\,{\rm M}_\odot/{\rm L}_\odot$. This high dynamical M/L along with a cuspy velocity dispersion profile in the DSC model can be explained as the result of the presence of an IMBH that significantly influences the internal kinematics of the cluster. In order to fully exclude the presence of a BH subsystem in NGC 6535, measurements of the central dispersion profile of NGC 6535 are needed that do not currently exist.

5.2 Observing the possible kinematic signature of an IMBH in NGC 6535

As mentioned earlier, existing searches for signatures of IMBHs using stellar kinematics yield controversial results. The largest discrepancy exists between the results obtained from integrated light measurements and resolved stars. A large part of this controversy can be attributed to our incomplete knowledge of the observed data, especially the PSF. The shape of the PSF determines how strongly bright stars contaminate the integrated light – as does it determine the fraction of flux contamination from nearby sources in spaxels that seem dominated by individual stars. Unfortunately, at least in ground-based observations, the PSF is not known a priori and has to be modelled from the data. The simulated data presented in the previous section have a known PSF, therefore they necessarily represent a simplification compared to real data. To maximize the reliability of kinematic measurements in the centres of GCs, one would ideally combine the results from individual stars and the integrated light. The inclusion of individual stars would also have the added advantage of potentially revealing other kinematical signatures of an IMBH, such as high-velocity stars orbiting in the direct vicinity of the BH that would be missed by integrated light analyses.

Proper motions as presented in Watkins et al. (2015) represent one possibility to obtain results from individual stars. However, as illustrated in Fig. 9, the existing data do not yet reach far enough into the cluster centre to get meaningful constraints on an IMBH. Alternatively, one may use radial velocities measured from the ground. Kamann, Wisotzki & Roth (2013) presented an approach to extract individual stellar spectra from IFU data via PSF fitting. Not only is this approach capable of suppressing contamination from nearby stars or unresolved light in the extracted spectra, but it also offers several advantages for the analysis of the integrated light from the same data. First, it provides an estimate of the shape of the PSF in the data. Secondly, it can be used to quantify atmospheric effects such as a change of the source positions due to atmospheric refraction. But most importantly, thanks to the knowledge of the PSF, the contributions of the resolved stars can be accurately subtracted from the data, allowing one to study the unresolved light free from their contamination.

[4] We caution that the value used for the virial mass estimate should correspond to the one calculated within the half-mass radius.

We ran the code of Kamann et al. (2013) on our SISCO simulation of the DSC. The full width at half-maximum of the PSF could be recovered to an accuracy of ∼1 per cent. In total, about 100 useful stellar spectra were extracted. We measured the velocities of these stars using the IRAF routine *fxcor* and compared them to the output of the simulation. Besides a few outliers due to unresolved binaries, the agreement was excellent, highlighting the potential of this approach.

An instrument that would allow the kinematics to be measured from the unresolved light and the resolved stars at the same time needs to combine a high spatial sampling with a high spectral resolution. At the European Southern Observatory VLT, ARGUS is the only instrument offering this combination. Besides, there are other integral field spectrographs that are not suited for integrated light analyses (because of their relatively low spectral resolution), but would enhance the possibilities for measuring stellar velocities. The AO-assisted IFU SINFONI is one such example (Eisenhauer et al. 2003); another one is MUSE (Bacon et al. 2010), the panoramic spectrograph recently installed at the VLT. As shown by Kamann et al. (2016), it allows the simultaneous observation of several thousand stars in the centres of GCs. Its upgrade with an AO system is foreseen for next year and will allow one to probe the kinematics around potential BHs in great detail.

6 CONCLUSIONS AND DISCUSSION

In this paper, we present a new class of star cluster models that emerged from results of thousands of star cluster simulations carried out using the MOCCA code for star cluster simulations as part of the MOCCA Survey I project. These particular DSC models form an IMBH via the scenarios explained in Giersz et al. (2015) within Hubble time and this IMBH makes up for more than 50 per cent of the cluster mass at 12 Gyr. Due to the low galactocentric radius values for these cluster models, the low-mass stars in the outer parts of the cluster rapidly escape due to tidal stripping. The cluster loses significant mass due to escaping stars and the internal dynamics of the cluster. Moreover, the formation of an IMBH and mass segregation also contribute to this process of sustained mass-loss due to escaping stars. The present day mass function for such star clusters is bottom-light.

The structural properties of some of these simulated DSC models (luminosity and radius) show similarities to a sample of low-luminosity Galactic GCs. Taking one of these star cluster models, we thoroughly analysed the photometric and kinematic properties of this model at Hubble time using the strategy of simulating realistic mock observations using the COCOA and SISCO codes. This allowed us to compare our DSC model with Galactic GCs and we found that the properties of NGC 6535 are the closest to our DSC model. If our DSC model and NGC 6535 had similar evolutionary histories, then it would make NGC 6535 a candidate for harbouring an IMBH. It needs to be stressed that the initial conditions for the models used in the MOCCA-Survey I were arbitrarily selected and were not tuned to reproduce particular clusters. Despite this, the agreement of the photometric and kinematic properties with NGC 6535 is remarkably good and suggests that this GC may have had a dynamical history similar to our DSC model and consequently, it may be harbouring an IMBH. Various observations also suggest that NGC 6535 has a very high M/L ratio value of around 11 (Zaritsky et al. 2014), which is the highest M/L ratio value for any Galactic GC. Its present-day mass function shows that there is a clear absence of low-mass stars (Halford & Zaritsky 2015), which clearly shows that the high M/L ratio cannot be attributed to a large number of low-mass stars in a scenario where the cluster may have had a bottom-heavy IMF. All these observations are in agreement with our DSC model and therefore there may be a large dark mass component in NGC 6535 in the form of an IMBH.

Future kinematic observations of the central areas of NGC 6535 could unveil a kinematic peak in the velocity dispersion, as predicted by our model. Most observational campaigns that search for kinematic signatures of IMBH in GCs have generally focused on very large and massive GCs. There are quite a few problems that can plague the results of such observations for very dense and crowded fields in massive clusters. However, if future campaigns do observe a kinematic peak in a small cluster like NGC 6535, then this would provide clear-cut evidence for the existence of an IMBH.

ACKNOWLEDGEMENTS

The authors would like to thank the referee for their insightful comments and useful suggestions. AA, MG and AH were partially supported by the Polish National Science Centre (PNSC) through the grant DEC-2012/07/B/ST9/04412. AA would also like to acknowledge support by the PNSC through the grant UMO-2015/17/N/ST9/02573 and partial support from Nicolaus Copernicus Astronomical Centre's grant for young researchers. PB acknowledges financial support from the International Max-Planck Research School for Astronomy and Cosmic Physics at the University of Heidelberg (IMPRS-HD). RdV acknowledges financial support from the Angelo Della Riccia foundation. SK received funding through BMBF Verbundforschung (project MUSE-AO, grant 05A14MGA).

REFERENCES

Amaro-Seoane P., Freitag M., Spurzem R., 2004, MNRAS, 352, 655
Anderson J., van der Marel R. P., 2010, ApJ, 710, 1032
Askar A., Giersz M., Pych W., Olech A., Hypki A., 2016, in Meiron Y., Li S., Liu F.-K., Spurzem R., eds, Proc. IAU Symp. 312, Star Clusters and Black Holes in Galaxies across Cosmic Time. Kluwer, Dordrecht, p. 262
Askar A., Szkudlarek M., Gondek-Rosińska D., Giersz M., Bulik T., 2017, MNRAS, 464, L36
Bacon R. et al., 2010, in McLean I. S., Ramsay S. K., Takami H., eds, Proc. SPIE Conf. Ser. Vol. 7735, Ground-based and Airborne Instrumentation for Astronomy III. SPIE, Bellingham, p. 773508
Bahcall J. N., Wolf R. A., 1976, ApJ, 209, 214
Banerjee S., Kroupa P., 2011, ApJ, 741, L12
Baumgardt H., Makino J., Ebisuzaki T., 2004a, ApJ, 613, 1133
Baumgardt H., Makino J., Ebisuzaki T., 2004b, ApJ, 613, 1143
Belczynski K., Kalogera V., Bulik T., ApJ, 572, 407
Bellini A. et al., 2014, ApJ, 797, 115
Belloni D., Giersz M., Askar A., Leigh N., Hypki A., 2016, MNRAS, 462, 2950
Bianchini P., Norris M. A., van de Ven G., Schinnerer E., 2015, MNRAS, 453, 365
Bianchini P., Norris M., van de Ven G., Schinnerer E., 2016, Meiron Y., Li S., Liu F.-K., Spurzem R., eds, Proc. IAU Symp. 312, Star Clusters and Black Holes in Galaxies Across Cosmic Time. Kluwer, Dordrecht, p. 223
Cappellari M., Emsellem E., 2004, PASP, 116, 138
de Vita R. et al., 2016, MNRAS, in press
Eisenhauer F. et al., 2003, in Iye M., Moorwood A. F. M, eds, Proc. SPIE Conf. Ser. Vol. 4841, Instrument Design and Performance for Optical/Infrared Ground-based Telescopes. SPIE, Bellingham, p. 1548
Ferrarese L., Merritt D., 2000, ApJ, 539, L9
Fregeau J. M., Cheung P., Portegies Zwart S. F., Rasio F. A., 2004, MNRAS, 352, 1
Fukushige T., Heggie D. C., 2000, MNRAS, 318, 753

Gebhardt K., Pryor C., O'Connell R. D., Williams T. B., Hesser J. E., 2000, AJ, 119, 1268
Gerssen J., van der Marel R. P., Gebhardt K., Guhathakurta P., Peterson R. C., Pryor C., 2002, AJ, 124, 3270
Gerssen J., van der Marel R. P., Gebhardt K., Guhathakurta P., Peterson R. C., Pryor C., 2003, AJ, 125, 376
Giersz M., Heggie D. C., Hurley J. R., Hypki A., 2013, MNRAS, 411, 2184
Giersz M., Leigh N., Hypki A., Lützgendorf N., Askar A., 2015, MNRAS, 454, 3150
Graham A. W., Scott N., 2015, ApJ, 798, 54
Gürkan M. A., Freitag M., Rasio F. A., 2004, ApJ, 604, 632
Halford M., Zaritsky D., 2015, ApJ, 815, 86
Harris W. E., 1996, AJ, 112, 1487
Heggie D. C., 2014, MNRAS, 445, 3435
Hénon M. H., 1971, Ap&SS, 14, 151
Holley-Bockelmann K., Mihos J. C., Sigurdsson S., Hernquist L., Norman C., 2002, ApJ, 567, 817
Hong J., Lee H. M., 2015, MNRAS, 448, 754
Hurley J. R., 2007, MNRAS, 379, 93
Hurley J. R., Pols O. R., Tout C. A., 2000, MNRAS, 315, 543
Hurley J. R., Tout C. A., Pols O. R., 2002, MNRAS, 329, 897
Kamann S., Wisotzki L., Roth M. M., 2013, A&A, 549, A71
Kamann S. et al., 2016, A&A, 588, A149
King I. R., 1966, AJ, 71, 64
Kroupa P., 2001, MNRAS, 322, 231
Lanzoni B. et al., 2013, ApJ, 769, 107
Lützgendorf N., Kissler-Patig M., Noyola E., Jalali B., de Zeeuw P. T., Gebhardt K., Baumgardt H., 2011, A&A, 533, A36
Lützgendorf N., Gebhardt K., Baumgardt H., Noyola E., Neumayer N., Kissler-Patig M., de Zeeuw T., 2015, A&A, 581, A1
Lützgendorf N. et al., 2016, in Meiron Y., Li S., Liu F.-K., Spurzem R., Proc. IAU Symp. 312, Star Clusters and Black Holes in Galaxies Across Cosmic Time. Kluwer, Dordrecht, p. 181
Madau P., Rees M. J., 2001, ApJ, 551, L27
Madrid J. P., Leigh N., Hurley J. R., Giersz M., 2016, MNRAS, in press
Magorrian J. et al., 1998, AJ, 115, 2285
Mapelli M., 2016, MNRAS, 459, 3432
Marín-Franch A. et al., 2009, ApJ, 694, 1498
Miller M. C., Hamilton D. P., 2002, MNRAS, 330, 232
Milone A. P. et al., 2012, A&A, 540, A16
Noyola E., Gebhardt K., 2006, AJ, 132, 447
Noyola E., Gebhardt K., Bergmann M., 2008, ApJ, 676, 1008-1015
Noyola E., Gebhardt K., Kissler-Patig M., Lützgendorf N., Jalali B., de Zeeuw P. T., Baumgardt H., 2010, ApJ, 719, L60
Paust N. E. Q. et al., 2009, AJ, 137, 246
Piotto G. et al., 2002, A&A, 391, 945
Portegies Zwart S. F., Baumgardt H., Hut P., Makino J., McMillan S. L. W., 2004, Nature, 428, 724
Rosenberg A., Piotto G., Saviane I., Aparicio A., 2000a, A&AS, 144, 5
Rosenberg A., Aparicio A., Saviane I., Piotto G., 2000b, A&AS, 145, 451
Sigurdsson S., Hernquist L., Quinlan G. D., 1995, ApJ, 446, 75
Stetson P. B., 1987, PASP, 99, 191
Stetson P. B., 1994, PASP, 106, 250
Stodółkiewicz J. S., 1986, Acta Astron., 36, 19
Stone N. C., Küpper A. H. W., Ostriker J. P., 2016, preprint (arXiv:1606.01909)
Strader J., Chomiuk L., Maccarone T. J., Miller-Jones J. C. A., Seth A. C., Heinke C. O., Sivakoff G. R., 2012, ApJ, 750, L27
Sun M.-Y., Jin Y.-L., Gu W.-M., Liu T., Lin D.-B., Lu J.-F., 2013, ApJ, 776, 118
Taylor M. A., Puzia T. H., Gomez M., Woodley K. A., 2015, ApJ, 805, 65
van der Marel R. P., Anderson J., 2010, ApJ, 710, 1063
Wang L. et al., 2016, MNRAS, 458, 1450
Watkins L. L., van der Marel R. P., Bellini A., Anderson J., 2015, ApJ, 803, 29
Wolf J., Martinez G. D., Bullock J. S., Kaplinghat M., Geha M., Muñoz R. R., Simon J. D., Avedo F. F., 2010, MNRAS, 406, 1220
Young P., 1980, ApJ, 242, 1232
Zaritsky D., Colucci J. E., Pessev P. M., Bernstein R. A., Chandar R., 2014, ApJ, 796, 71

This paper has been typeset from a TEX/LATEX file prepared by the author.